Swiss J Geosci (2017) 110:677–697
DOI 10.1007/s00015-017-0270-7

Along-strike shear-sense reversal in the Vals-Scaradra Shear Zone at the front of the Adula Nappe (Central Alps, Switzerland)

Jacek Kossak-Glowczewski[1] · Nikolaus Froitzheim[1] · Thorsten Nagel[2] · Jan Pleuger[3] · Ruth Keppler[1] · Bernd Leiss[4] · Verena Régent[5]

Received: 26 July 2016 / Accepted: 16 March 2017 / Published online: 5 April 2017

Abstract The Adula Nappe in the Central Alps comprises pre-Mesozoic basement and minor Mesozoic sediments, overprinted by Paleogene eclogite-facies metamorphism. Peak pressures increase southward from ca. 1.2 GPa to values over 3 GPa, which is interpreted to reflect exhumation from a south-dipping subduction zone. The over- and underlying nappes experienced much lower Alpine pressures. To the north, the Adula Nappe ends in a lobe surrounded by Mesozoic metasediments. The external shape of the lobe is simple but the internal structure highly complicated. The frontal boundary of the nappe represents a discontinuity in metamorphic peak temperatures, between higher T in the Adula Nappe and lower T outside. A shear zone with steeply dipping foliation and shallowly-plunging, WSW-ENE oriented, i.e. orogen-parallel stretching lineation overprinted the northernmost part of the Adula Nappe and the adjacent Mesozoic metasediments (Vals-Scaradra Shear Zone). It formed during the local Leis deformation phase. The shear sense in the Vals-Scaradra Shear Zone changes along strike; from sinistral in the W to dextral in the E. Quartz textures also vary along strike. In the W, they indicate sinistral shearing with a component of coaxial (flattening) strain. A texture from the middle part of the shear zone is symmetric and indicates coaxial flattening. Textures from the eastern part show strong, single c-axis maxima indicating dextral shearing. These relations reflect complex flow within the Adula Nappe during a late stage of its exhumation. The structures and reconstructed flow field indicate that the Adula basement protruded upward and northward into the surrounding metasediments, spread laterally, and expelled the metasediments in front towards west and east.

Keywords Central Alps · Northern Adula Nappe · Exhumation · Vals-Scaradra Shear Zone · Quartz textures

1 Introduction

The Adula Nappe in the Eastern Central Alps (Switzerland and Italy) is a classical area of eclogite-facies metamorphism and ideally suited for studies of high-pressure rock exhumation. The eastward tilting of the thrust sheets in this area and erosion have resulted in a situation whereby the entire HP-UHP unit, ca. 45 km long in N–S direction (Fig. 1), is accessible and well-exposed, including the sole, roof, front, and root of the nappe. Geology, petrology, and geochronology of the Adula Nappe have been the subject of many detailed studies (e.g., Jenny et al. 1923; Heinrich 1986; Löw 1987; Nagel et al. 2002a, b; Pleuger et al. 2003; Dale and Holland 2003; Zulbati 2008, 2011; Liati et al. 2009; Sandmann et al. 2014; Cavargna-Sani et al. 2014a, b) but the mechanism of its exhumation from HP-UHP depth is still not well understood and exhumation models face kinematic problems. Most notably, reconstructions of the

Editorial handling: S. Schmid.

✉ Jacek Kossak-Glowczewski
jacekkossak@gmx.de

[1] Steinmann-Institut, Universität Bonn, Poppelsdorfer Schloss, 53115 Bonn, Germany

[2] Department of Geoscience, Aarhus University, Høgh-Guldbergs Gade 2, 8000 Aarhus C, Denmark

[3] Institut für Geologische Wissenschaften, Freie Universität Berlin, Malteserstrasse 74-100, 12249 Berlin, Germany

[4] Geoscience Zentrum der Universität Göttingen, Goldschmidtstraße 3, 37077 Göttingen, Germany

[5] Geo Center Møns Klint, Stengårdsvej 8, 4791 Borre, Denmark

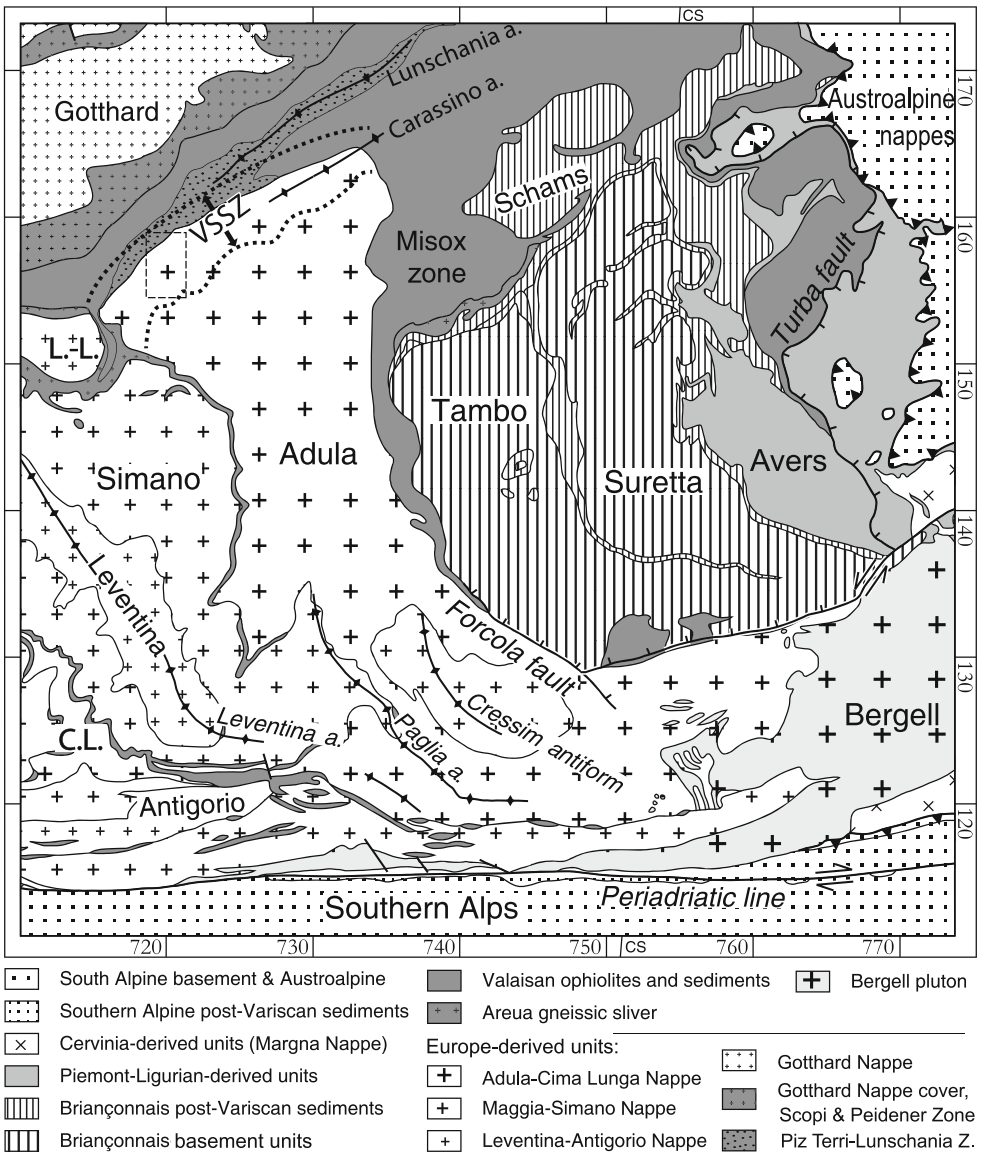

Fig. 1 Tectonic map of the Lepontine nappe stack (after Pleuger et al. 2008). Note eastward tilting of the thrust sheets. *CL* Cima Lunga Nappe, *L-L* Lucomagno-Leventina Nappe, *VSSZ* Vals-Scaradra Shear Zone. *Rectangle* shows the position of the map in Fig. 3

exhumation process imply top-south directed shearing along the roof of the Adula Nappe at some stage (Schmid et al. 1996, Froitzheim et al. 2003). Mylonites indicating top-south shearing, however, have not been found. Therefore it has been suggested that the high metamorphic pressures in the Adula Nappe do not reflect subduction to mantle depth but tectonic overpressure (Pleuger and Podladchikov 2014). On the other hand, the Adula Nappe not only exhibits much higher metamorphic pressures than the surrounding tectonic units but also very distinctive structural features, for example a rather complicated internal structure that is in contrast to its simple external shape (Fig. 2). This has led some authors to describe the Adula Nappe as a composite of tectonic slivers formed in a "Paleogene Tectonic Accretion Channel" (Berger et al. 2005).

In this article, we present the results of geological mapping in the area of Val Scaradra, together with the microstructure and texture of quartz mylonites from the newly defined Vals-Scaradra Shear Zone, i.e. along the northern border of the Adula Nappe. This shear zone is remarkable in that it exhibits a reversal of shear sense along strike. We think that it is a key element for reconstructing the tectonic evolution of the Adula Nappe.

2 Regional geology of the Adula Nappe

The bulk of the Adula Nappe is formed by SiO_2-rich para- and orthogneiss from Cambrian, Ordovician, and Permian protoliths (Cavargna-Sani et al. 2014a) with lenses of eclogite, variably retrogressed to amphibolite, and some lenses of peridotite, partly garnet bearing, in the southern part. Layers of quartzite and marble are found locally along the borders of the Adula Nappe. Quartzite and marble are

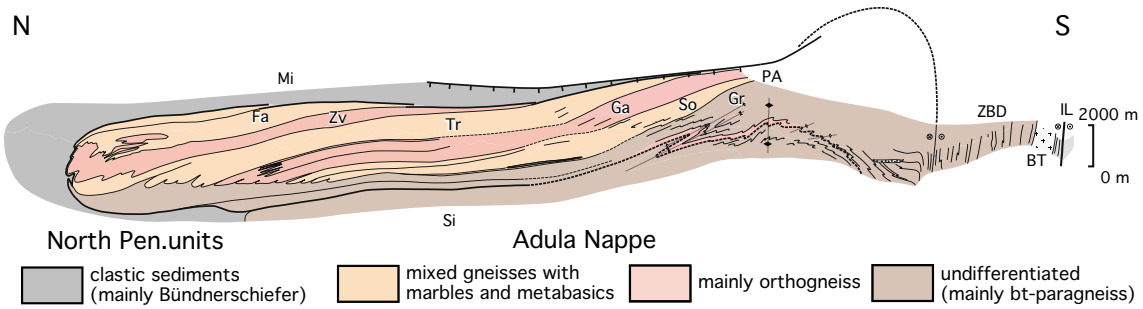

Fig. 2 N–S cross-section through the Adula Nappe with its tectonic subdivision (after Nagel 2008): Fa, Fanella Lobe; Ga, Ganan Lobe; Gr, Groveno Lobe; IL, Insubric Line; Mi, Misox Zone; PA, Paglia Antiform; Si, Simano Nappe; So, Soazza Lobe; Tr, Trescolmen Lobe; ZBD, Zone of Bellinzona-Dascio; Zv, Zervreila Lobe; BT, Bergell Tonalite

also found inside the Adula Nappe, complexly folded together with the gneissic rocks ("Internal Mesozoic"; Fig. 3). These represent the former Mesozoic sedimentary cover of the Adula basement (Cavargna-Sani et al. 2010). In spite of extreme ductile deformation, transgressive contacts between the "Internal Mesozoic" and the basement are still visible (Cavargna-Sani et al. 2014b). According to these authors, the Mesozoic sedimentary rocks surrounding the Adula Nappe are everywhere in tectonic contact with the basement rocks, except at the base of the nappe in its northwestern part, where the contact is stratigraphic, showing that this area represents the inverted limb of a fold nappe.

Although neither coesite nor diamond have been found so far, there is compelling evidence that garnet peridotite and eclogite bodies in the southern part of the nappe (e.g. at Alpe Arami) experienced UHP conditions, with pressures reaching at least 3.2 GPa at 840 °C (Nimis and Trommsdorff 2001), possibly as much as ca. 5 GPa at 1120 °C (Brenker and Brey 1997). The peak pressure conditions decrease northward (Heinrich 1986). This is generally interpreted as reflecting a southward dip of the subduction zone into which the rocks descended during the Alpine orogeny (e.g., Dale and Holland 2003). Both Alpine and Pre-Alpine (Variscan) ages have been determined for the high-pressure metamorphism in the Adula Nappe (Becker 1993; Gebauer 1996; Brouwer et al. 2005; Liati et al. 2009; Herwartz et al. 2011). Sandmann et al. (2014) showed that the UHP metamorphism in the southern part is Eocene in age (ca. 35–38 Ma) and has wiped out any signs of Variscan metamorphism. Towards the north, as the grade of Alpine metamorphism decreases, remnants of Variscan garnet occur in the cores of Alpine garnet, and both can be dated in one and the same sample using Lu-Hf chronometry (Herwartz et al. 2011; Sandmann et al. 2014). In the northernmost part of the nappe, garnet in eclogites is entirely Variscan (ca. 330 Ma), which makes it very likely that the basement of the Adula Nappe already contained Variscan eclogite or garnet amphibolite before it was subducted in the Eocene.

Table 1 Deformation phases in the Adula Nappe after Löw (1987), Meyre and Puschnig (1993), Nagel et al. (2002a), and Cavargna-Sani et al. (2014b)

	Northern Adula	Middle Adula	Southern Adula
30–20 Ma	*Carassino*	–	*Cressim*
35–30 Ma	*Leis*	(*Leis*)	*Claro*
	Zapport		
40–35 Ma	*Sorreda/Ursprung*	*Trescolmen*	–

The structure of the Adula Nappe is dominated by a pronounced foliation subparallel to the base and top of the nappe, N–S oriented isoclinal folds, partly with a sheath-fold geometry, and an equally N–S oriented stretching lineation associated with shear-sense criteria showing top-to-the-north transport (Zapport Phase; Löw 1987; Table 1). Along the northern front of the nappe, however, a strong stretching lineation occurs that is orientated WSW–ENE, strongly oblique to the Zapport lineation. It is found on a foliation, which is axial planar to folds deforming the Zapport-Phase folds. These younger folds, as well as associated foliations and stretching lineations belong to the Leis Phase (Löw 1987). Both Zapport and Leis structures are related to the exhumation of the nappe (Löw 1987). Structures older than the Zapport Phase comprise (1) eclogite-facies foliations and stretching lineations in eclogite bodies (Trescolmen Phase; Meyre and Puschnig 1993) and (2) the alternation of layers of basement and "Internal Mesozoic", together with a first foliation parallel to the lithological contacts. Löw (1987) assumed that the alternation resulted from thrust imbrication that occurred during his Sorreda Phase. Cavargna-Sani et al. (2014b), however, found that the alternation resulted from isoclinal folding of stratigraphic basement-cover contacts and introduced the term Ursprung Phase for these same structures. The recognition of pre-Zapport isoclinal folding is important because it underlines that the Adula Nappe, though extremely deformed, is rather a coherent unit than a mélange of tectonic lenses as previously suggested

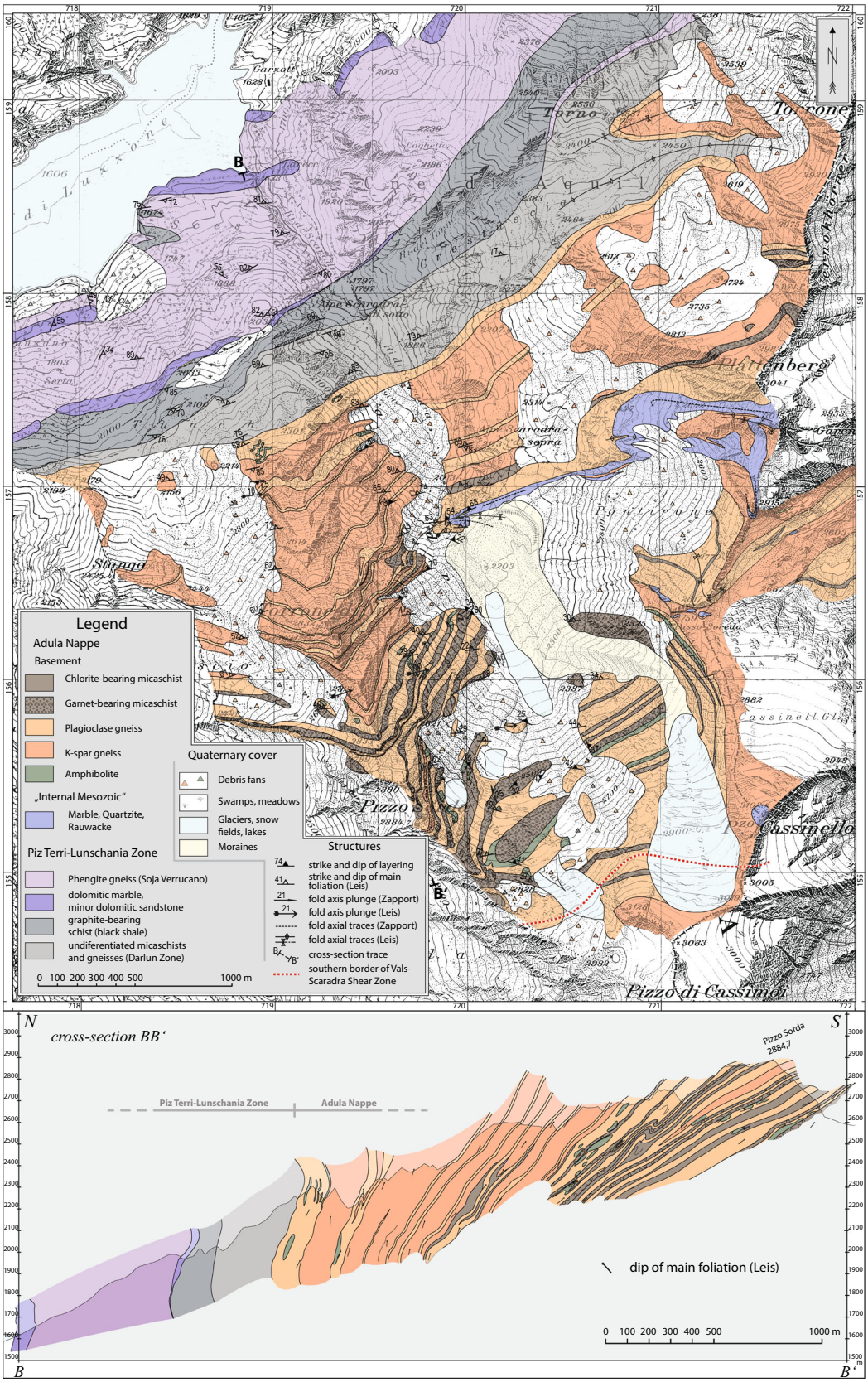

Fig. 3 Above: Geological map of Val Scaradra showing the northwestern front of the Adula Nappe and the metasedimentary rocks bordering it to the north. Below: *Cross-section* through the map area

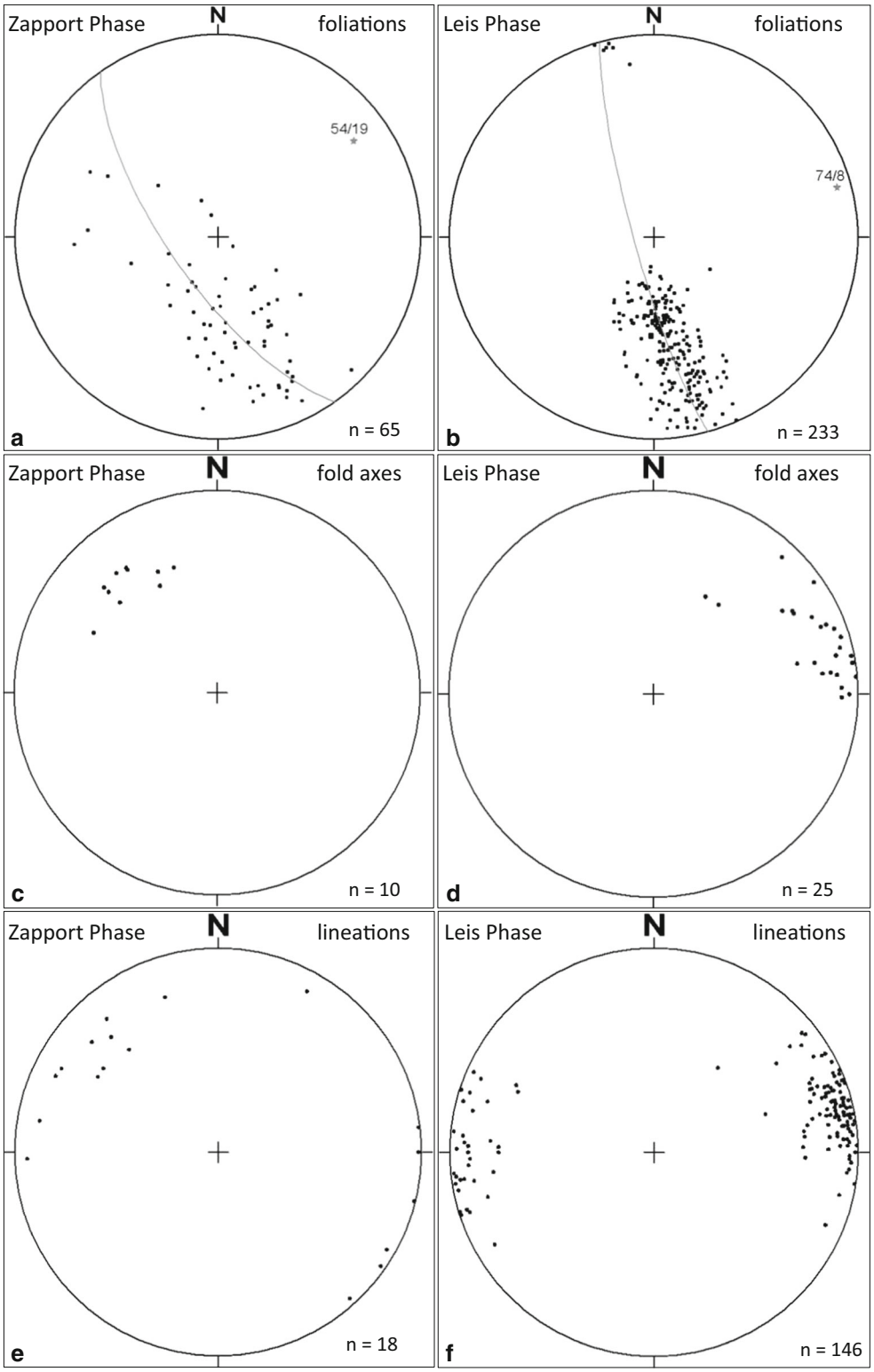

Fig. 4 Schmidt nets of structural elements, lower hemisphere. **a** Distribution of Zapport foliations on a great circle points to main fold axis orientation of the Leis Phase (FA 054/19). This is parallel to measured fold axes shown in (**d**). **b** Poles of main foliation (Leis Phase). The pole of the great *circle* dipping shallowly to the ENE suggests a fold axis of the younger D3 (Carassino Phase, FA 074/08). **c** Measured fold axes related to the Zapport Phase. **d** Measured fold axes related to the Leis Phase. **e** Mineral lineations defined by amphibole and feldspar in massive K-feldspar augengneiss, related to the Zapport Phase. **f** Stretching lineation of the Leis Phase, defined by chlorite, white mica and quartz

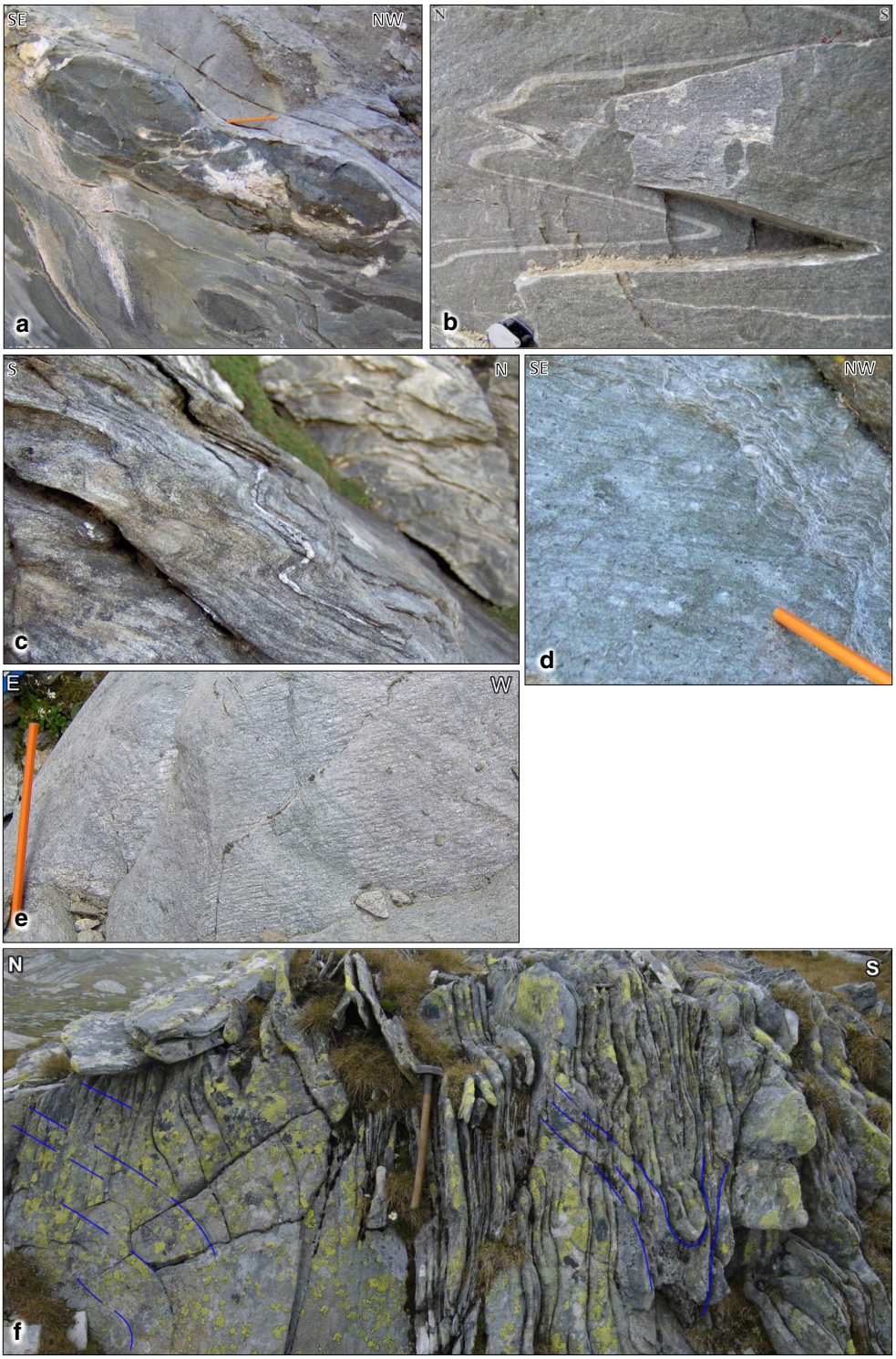

(Trommsdorff 1993; Brouwer et al. 2005). Since in our opinion the new interpretation of the Sorreda-Phase structures does not require a new name we will use the original name Sorreda Phase in the following for this first phase of isoclinal folding. It is not known if the Trescolmen Phase, i.e. the eclogite-facies deformation, and the Sorreda Phase, i.e. the "mixing" of basement and sediments, are of the same or of a slightly different age.

Leis-Phase structures in the northern part of the Adula Nappe are overprinted by a large north-closing antiform with a south-dipping axial plane. This leads to a northward steepening of the older foliations (Fig. 3). This antiform

◀**Fig. 5** Structural outcrop observations: **a** Boudins of amphibolite in gneiss, wrapped by the Zapport foliation, in the southern part of the mapping area (R: 719,780, H: 155,660). Quartz-filled boudin necks indicate roughly NW–SE stretching (parallel to the outcrop surface). **b** Massive plagioclase gneiss from 0.5 km to the south of Alpe Scaradra di sopra (R: 720,558, H: 155,538), showing lithological layering corresponding to the Zapport foliation. This foliation has been folded into tight folds of the Leis Phase. Leis-fold axis plunges northeast (035/45). **c** Amphibole-bearing plagioclase gneiss (R: 719,792, H: 155,642) exhibits parasitic folding (3-rd order) of Leis Phase. Fold axis: 091/09, fold axial plane: 013/39. **d** Zapport-Phase foliation plane in K-feldspar augen gneiss with stretching lineation (306/31) defined by elongate K-feldspar porphyroclasts and aggregates. Locality: R: 719,775 H: 155,680. **e** Foliation plane (353/35) of the Leis-Phase crenulated by the Carassino Phase. Crenulation axes plunge east (080/03) parallel to the large-scale fold axis (cf. Fig. 4d). Locality: (R: 720,235, H: 155,756). **f** K-feldspar augengneiss north of Plattenberg, east of Torno. Leis foliation (*vertical*) overprints Zapport foliation (*blue lines*) and becomes more penetrative from *left* to *right*. A tight Leis fold is seen to the *right*

and parasitic folds are attributed to the Carassino Phase (Löw 1987). In the southern part of the Adula Nappe, the Zapport-Phase foliation was overprinted first by recumbent folds related to extensional shearing (Claro Phase) and then by upright folds (Cressim Phase, Nagel et al. 2002a).

The northern part of the Adula Nappe is overlain and enveloped by thrust sheets and slivers of Mesozoic (and minor Permian) metasedimentary rocks together with some lenses of basement gneiss and some metaophiolites. The part that lies on top of the nappe is known as the Misox Zone. The part along the front of the nappe includes a variety of units known as Lower and Upper Vals Slices, Aul Nappe, Piz Terri-Lunschania Zone, Soja Nappe, etc. (Voll 1976; Probst 1980; Wiederkehr et al. 2008, 2009, 2011; Galster et al. 2010, 2012). These units are partly derived from the southern margin of the European continent and partly from the oceanic Valais basin. The units in front of the Adula Nappe show four phases of penetrative deformation (named D1–D4; Wiederkehr et al. 2008). D4 is related to backfolding, D3 is related to northwest-vergent "forward" folding (Lunschania Antiform; Fig. 1) and is correlated with the Carassino Phase in the Adula Nappe, D2 is a folding and shearing event accompanied by isothermal decompression and probably contemporaneous with the Leis Phase in the Adula Nappe, and D1 represents folding and top-north shearing during subduction.

Wiederkehr et al. (2011) mapped peak metamorphic temperatures around the front of the Adula Nappe using Raman spectroscopy of carbonaceous material. They found that in the southwestern part of the nappe front, peak temperatures result from Miocene heating during the "Lepontine event" at ca. 20–18 Ma. In the northeastern part of the nappe front, however, peak metamorphic temperatures are older. They were reached during the Eocene subduction-exhumation cycle, between 42 and 35 Ma, and the isotherms of peak metamorphism in Mesozoic rocks outside the Adula Nappe were deformed by the local D3 folds (e.g., the Lunschania Antiform). These folds are assumed to be of the same age as the Carassino Phase within the Adula Nappe (Wiederkehr et al. 2008). In this northeastern area, there is a discontinuity in peak metamorphic temperature across the front of the Adula Nappe, from 500–525 °C in the Adula Nappe to 400–425 °C in the Mesozoic rocks bordering the Adula Nappe. On both sides of the discontinuity, these temperatures were reached during the Paleogene cycle.

The Vals-Scaradra Shear Zone includes that part of the Adula Nappe where the WSW-ENE lineation is predominant, as well as the southern part of the adjacent metasediments (Fig. 1).

3 Local geology of Val Scaradra

The area of Val Scaradra in the western part of the Adula Nappe front was mapped at the scale of 1:10,000 (Fig. 3). In this area, the basement rocks of the Adula Nappe comprise various types of gneiss (both ortho and para), mica schist, and amphibolite. Folded layers of quartzite, marble, and rauhwacke represent the "Internal Mesozoic". The general dip direction of the gneiss foliation is NNW, except in fold hinges, and the dip becomes steeper towards the nappe front. At the front, the gneiss does not carry a sediment cover but is overlain by an imbricate zone comprising lenses of gneiss, mica schist, carbonate- and graphite-bearing mica schist ("Bündnerschiefer"), and scattered greenschists. A mostly coherent layer of chlorite-sericite schist and quartzite occurs within this imbricate zone. These lithologies are interpreted as a metamorphic equivalent of the Late Triassic Quartenschiefer of the Helvetic nappes. This particular domain is called Darlun Zone by Probst (1980) and is part of the Piz Terri-Lunschania Zone. Towards northwest, the Darlun Zone is followed by homogenous carbonate- and graphite-bearing schist (Jurassic), marble (Triassic), and phengite gneiss, partly with deformed quartz pebbles (Permian). These units of the Piz Terri-Lunschania Zone represent the sedimentary cover of the Soja Nappe (Probst 1980) and exhibit the structure of an anticline, the Lunschania Antiform, with the phengite gneiss ("Soja Verrucano") in the core.

4 Structures within the Adula Nappe in Val Scaradra

Open, gentle folding during the Carassino Phase caused the general northward steepening of foliations, between shallowly north- to northwest-dipping in the southernmost part and vertical, WSW–ENE-striking at the front of the Adula

Nappe. This is illustrated by the Schmidt projection of the Leis-Phase foliation poles showing an incomplete great-circle distribution (Fig. 4b). The pole to this great circle represents the Carassino fold axis, which plunges shallowly east-northeast (074/08). Leis-Phase foliations were locally crenulated by the Carassino Phase (Fig. 5e). The crenulation axes are oriented parallel to the large-scale fold axis.

Structures of the Leis Phase comprise folds, foliation, and stretching lineation. The folds are open to tight (Fig. 5b, c) and their axes plunge shallowly to moderately east to northeast (Fig. 4d). The Leis foliation is axial planar with respect to these folds. It is the dominant foliation in most of the mapped area but with a tendency to decrease in intensity southward. To the south, anastomosing Leis-Phase shear zones enclose lenses with preserved older structures. The northern boundary of the Adula Nappe is parallel to the Leis foliation except north of Plattenberg where it is deformed by a downward-vergent antiform-synform pair of the Leis Phase (Fig. 3). The Leis foliation bears a stretching lineation mostly defined by dynamically recrystallized quartz and by stretched aggregates of chlorite, white mica, and epidote. The stretching lineation is approximately parallel to the fold axes (Fig. 4d, f). On rock surfaces parallel to the stretching lineation and perpendicular to the foliation, the sense of shear is sinistral (where the foliation is vertical) or top-west (where the foliation dips north), as indicated by asymmetric porphyroclast systems.

Folds of the Zapport Phase are preserved in Leis-Phase fold hinges and in lenses between Leis-Phase shear zones (Fig. 6). The folds are tight to isoclinal and the axes mostly plunge northwest (300°–330°) at moderate angles (Fig. 4c). The Zapport-Phase foliation is axial planar to these folds.

Fig. 7 Internal structure of the Adula Nappe on the western flank of Plattenberg. Outcrop pattern of "Internal Mesozoic" (*light blue*) and gneissic rocks (*grey*) reflects overprinting of Zapport, Leis and Carassino Phase. **a** Interference of Zapport and Leis folds. **b** Zapport-phase sheath fold with a N-plunging fold axis. **c** Entire west flank of Plattenberg. **d** Lithological boundaries and interpreted fold axial traces

Zapport-Phase foliation poles are distributed along a great circle indicating a northeast-plunging fold axis (054/19, Fig. 4a). This direction is parallel to Leis-Phase fold axes measured in the field (Fig. 4d). In hinges of Zapport-Phase folds, an older foliation is locally preserved. The Zapport-Phase foliation bears a stretching lineation typically defined by stretched K-feldspar porphyroclasts and aggregates and by elongate amphibole grains and aggregates (Fig. 5d). Boudinage of amphibolite lenses embedded in gneiss reflects extension parallel to the stretching lineation (Fig. 5a). The stretching lineation is subparallel to the fold axes and therefore oblique to perpendicular with respect to the Leis-Phase stretching lineation and fold axes (Fig. 4e).

The older foliation in the hinges of Zapport-Phase folds probably represents the Sorreda Phase (Löw 1987). Pre-Zapport fold hinges were not observed in the mapping area but duplicated layers in some places suggest the existence of pre-Zapport isoclinal folds (Fig. 6). Overprinting between these four ductile deformation phases explains the complicated outcrop pattern on the western flank of Plattenberg (Fig. 7).

Löw (1987) determined metamorphic peak conditions of ca. 470–540 °C and 1.2–1.5 GPa in the northern Adula Nappe. The temperatures were confirmed by Wiederkehr et al. (2011) who determined 500–520 °C using Raman spectroscopy of carbonaceous "Internal Mesozoic".

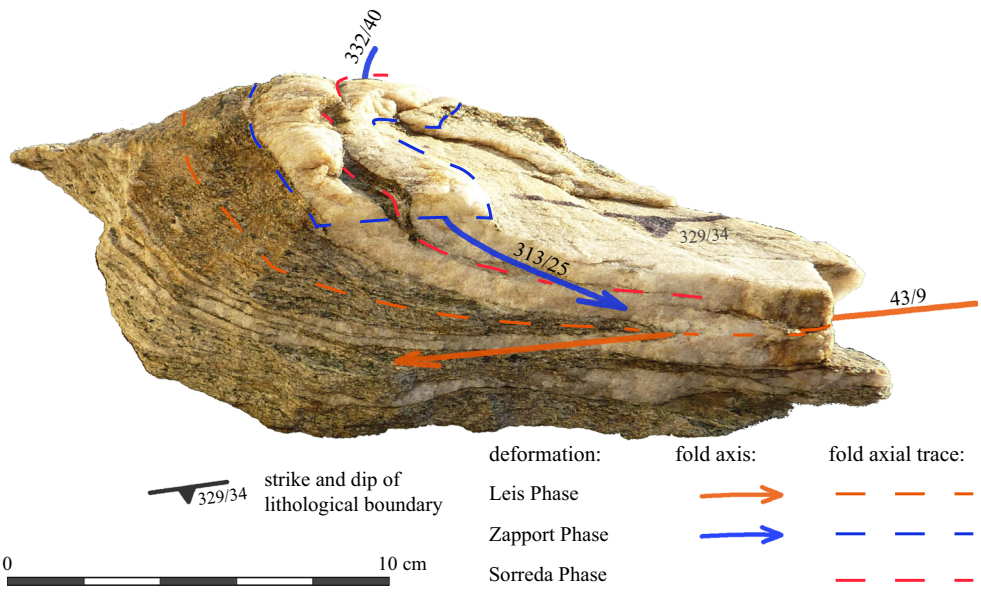

Fig. 6 Overprinting relations in a piece of chlorite-bearing mica schist with quartz veins (Adula-Nappe basement, R: 720,151, H: 156,109). Duplicated layer in the hinge of Zapport-phase fold suggest the existence of pre-Zapport isoclinal folds (Sorreda Phase)

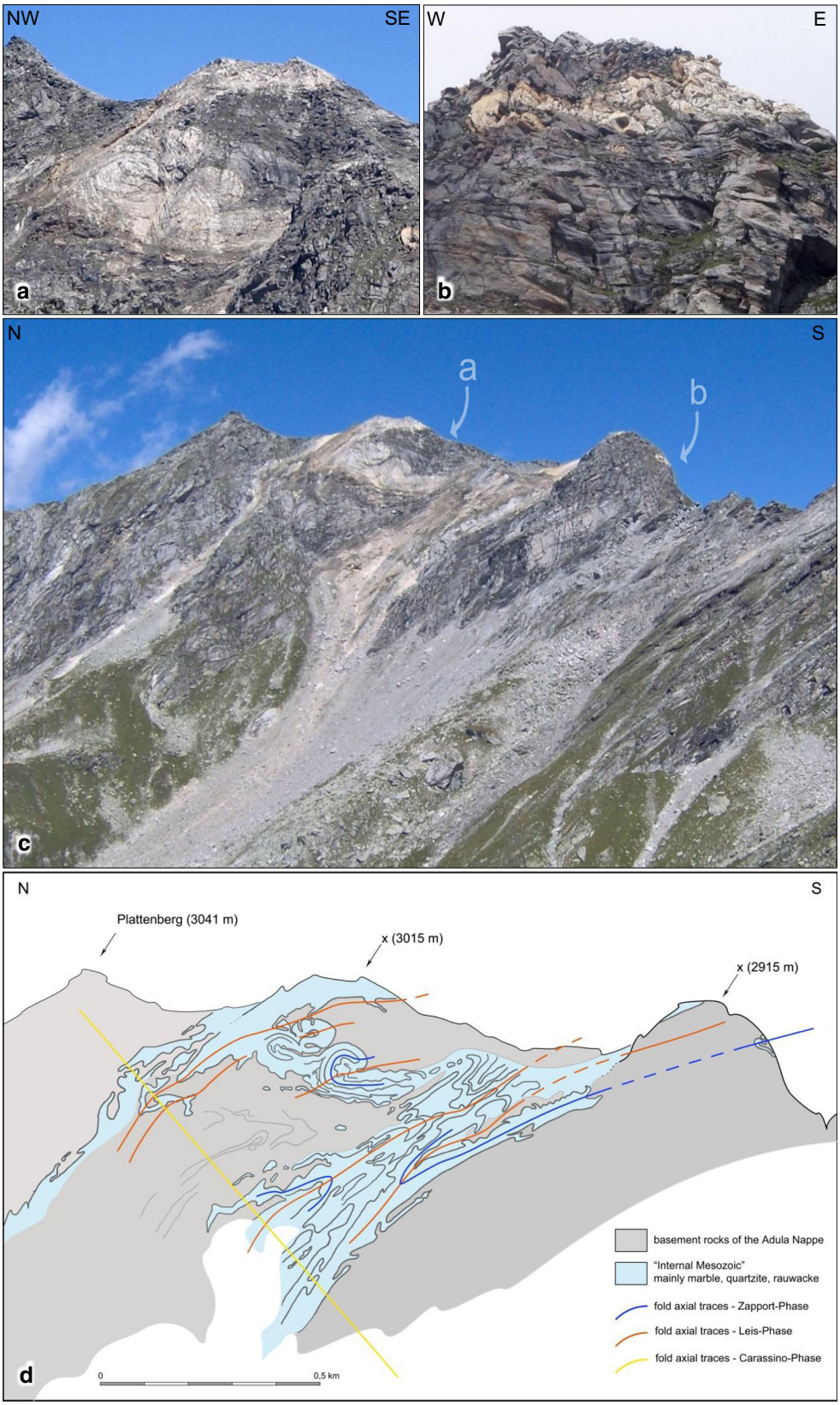
NW
SE
a
W
E
b
N
S
a
b
c
N
S
Plattenberg (3041 m)
x (3015 m)
x (2915 m)
basement rocks of the Adula Nappe
"Internal Mesozoic"
mainly marble, quartzite, rauwacke
fold axial traces - Zapport-Phase
fold axial traces - Leis-Phase
fold axial traces - Carassino-Phase
0
0,5 km
d

During the Zapport Phase, pressure decreased from the peak pressure to 0.8 GPa while T remained close to 500 °C, i.e., decompression was isothermal. The Leis Phase took place during further decompression under a pressure of ca. 0.7 GPa and still similar temperature (Löw 1987).

Thin sections of rocks from Val Scaradra show variably intense overprinting by the Leis Phase. In mica schists of the Adula-Nappe basement, the Leis foliation is defined by alternating chlorite-rich and white-mica-rich layers (Fig. 8b). Within the mica-rich layers, white mica grains partly preserve an oblique orientation, inherited from the

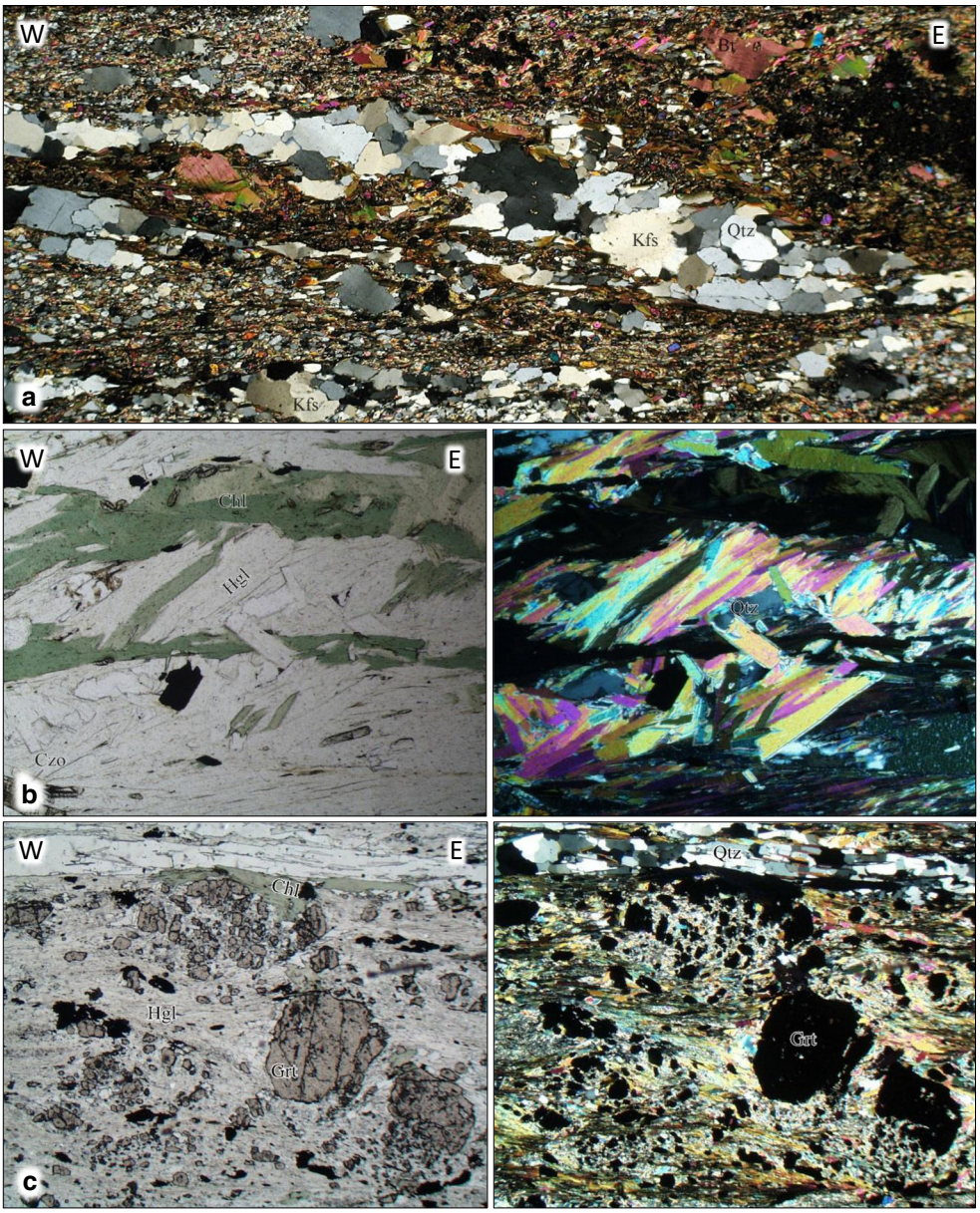

Fig. 8 Thin section observations from the Adula Nappe basement. All sections are parallel to the stretching lineation of the Leis Phase. **a** Strongly foliated K-feldspar augen gneiss. Sinistral shear sense (top-to-the-west) is indicated by large quartz-feldspar aggregate forming a σ-type porphyroclast system. Width of thin section: 4.7 mm; crossed polarizers. **b** Chlorite-bearing micaschist. Spaced foliation of the Leis-Phase is defined by *horizontal* cleavage domains consisting of chlorite aggregates. Oblique orientation of white mica grains in mica-rich microlithons represents cleavage of the earlier Zapport-Phase, kinked by the Leis Phase. Width of thin section: 1.7 mm; plane-polarized light (*left*) and crossed polarizers (*right*). **c** Garnet bearing micaschist. σ-type garnet porphyroclast in a matrix of white mica, quartz and epidote indicates top-west shear sense of Leis phase. Width of thin section: 6.9 mm; plane-polarized light (*left*) and crossed polarizers (*right*)

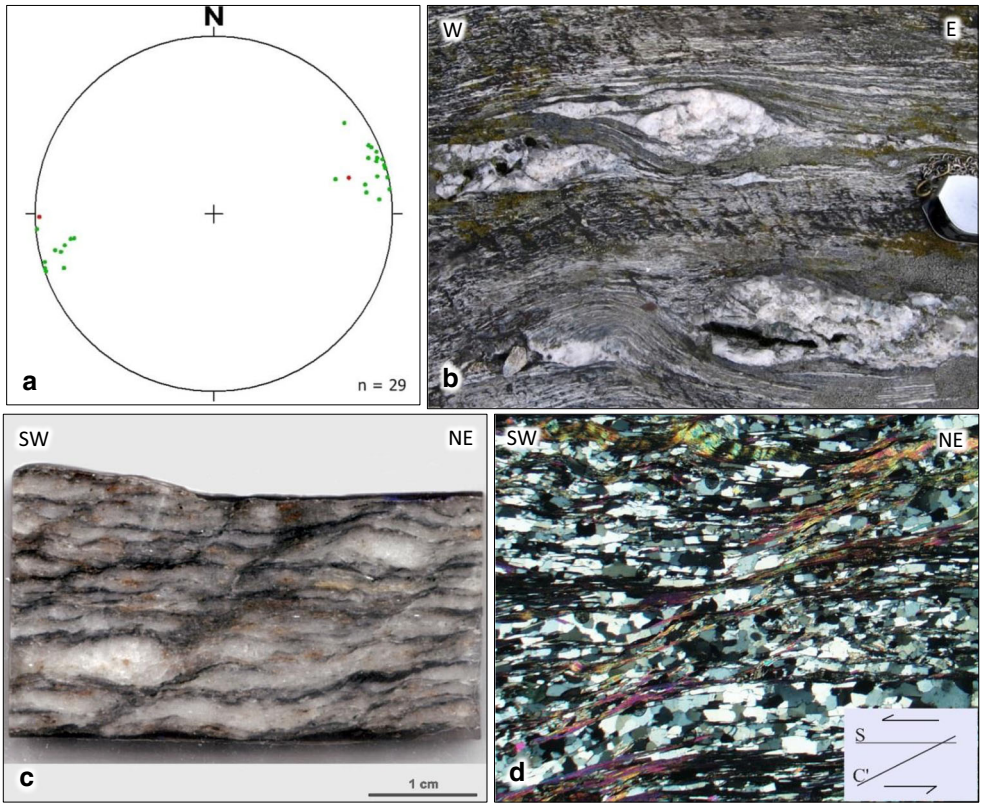

Fig. 9 Structural observations and data from the Piz Terri-Lunschania Zone in the Val Scaradra region. **a** Distribution of measured stretching lineations (*green marks*) and fold axes (*red marks*) of the D2 phase. **b** Phengite gneiss 0.5 km west of Alpe Scaradra di sotto (R: 718,940, H: 157,876). View of the X–Z plane of D2 (Leis Phase). σ-type quartz porphyroclasts in a phengite-rich matrix point to sinistral (*top*-W) shear sense. **c** Phengite gneiss with C′- type shear bands indicating sinistral shear sense (width of sample 5 cm). **d** Thin section of mylonitic phengite gneiss (R: 719,228, H: 158,155) under crossed polarizers cut parallel to X–Z plane of the D2 phase (foliation 342/81, stretching lineation 066/28, width of thin section 6.9 mm). Components are mainly quartz and phengite. C′- type shear band points to top-SW shear sense. Triple junctions of quartz grain boundaries indicate post-kinematic annealing similar to sample VF41

older Zapport Phase, and are kinked by Leis-Phase deformation (Fig. 8b). In garnet-bearing micaschists and K-feldspar augen gneisses, sinistral (top-west) shear sense is indicated by asymmetric pressure shadows of garnet (Fig. 8c) and K-feldspar or K-feldspar/quartz aggregates (Fig. 8a). Clear-cut shear bands were not observed.

5 Structures of the enveloping metasediments (Piz Terri-Lunschania Zone)

In the Val Scaradra area, units north of the Adula-Nappe basement are strongly affected by Leis-Phase deformation. The penetrative foliation can be traced across tectonic boundaries from gneisses of the Adula Nappe through the schistose metasediments of the Darlun Zone into the phengite gneisses in the core of the Piz Terri-Lunschania Zone. This Leis-related foliation corresponds to D2 of Wiederkehr et al. (2008). The foliation is axial planar with respect to tight folds with shallowly ENE-plunging fold axes. The stretching lineation has the same orientation (Fig. 9a). The shear sense is consistently sinistral, indicated by porphyroclasts and shear bands at outcrop- and thin-section scale (Fig. 9b, c, d). Shear-sense indicators are more abundant and clearer than within the Adula-Nappe basement, which suggests a northward increase in the rotational component of deformation.

6 Eastern part of the Vals-Scaradra Shear Zone

At the type-locality Leis near Vals, in ortho- and paragneisses of the northeasternmost part of the Adula Nappe, tight to isoclinal Leis-Phase folds with axial planar cleavage deform the Zapport foliation and refold Zapport-Phase folds. A pronounced stretching lineation, formed during the Leis Phase, is parallel to the fold axes. Both plunge shallowly northeast (Fig. 10b). The axial surfaces of the folds are parallel to the top boundary of the Adula Nappe, and the intensity of the Leis-

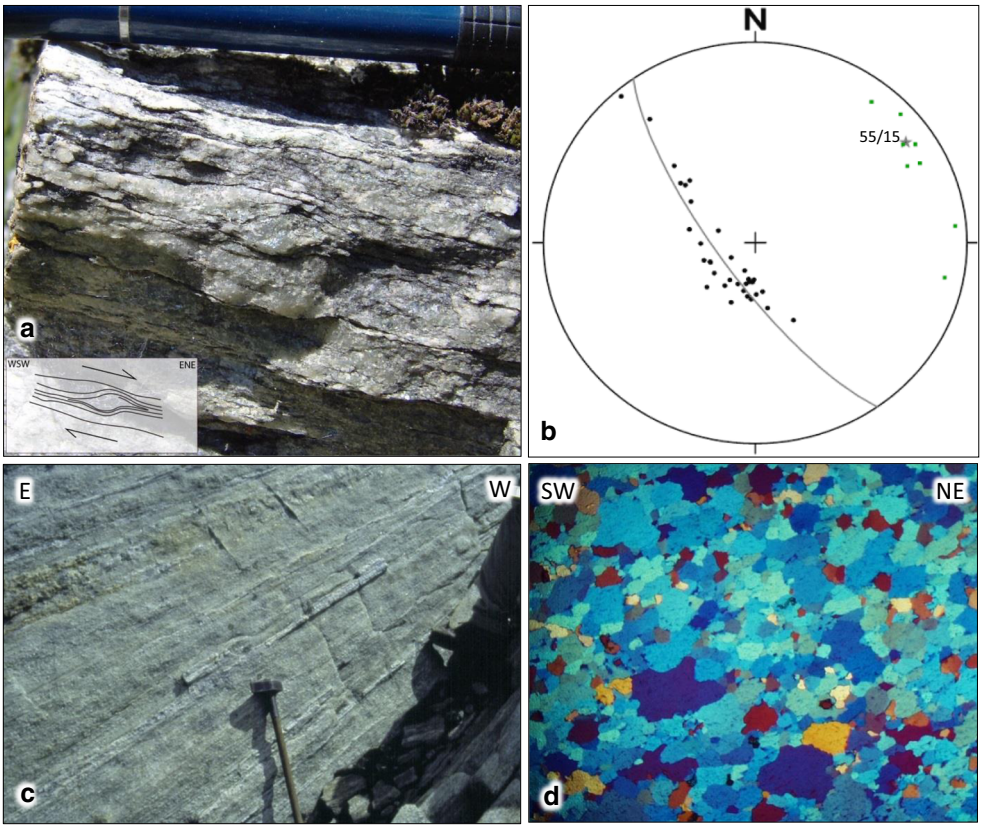

Fig. 10 Structural observations and data from the Vals region between Leis and Zervreila Lake. **a** Gneiss with quartz veins (R: 731,992, H: 163,408). View of the X–Z plane of the Leis-Phase deformation (foliation 070/21, stretching lineation 055/16). Polycrystalline quartz aggregates have sigmoidal shape indicating dextral (top-to-the-NE) shear sense. **b** Stereoplot of Zapport foliation poles (*black dots*) on a great *circle* indicating fold axis orientation of the Leis phase (fold axis 055/15). This is similar to the orientation in Val Scaradra region (Fig. 4). Measured stretching lineations (*green dots*) also dip shallowly to the NE and belong to the Leis phase. **c** Orthogneiss at the front of the Adula Nappe at Fuorcla da Puozas, north of Lake Zervreila. The foliation, forming the outcrop surface, is oriented 345/52 and the obvious, strong stretching lineation 067/10. Both represent the Leis Phase. View towards south. **d** Thin section of quartz vein taken to the north of Zervreila Lake (F 033/18, L 053/11). Thin section (with crossed polarizers and gypsum plate inserted, width of thin section 6.9 mm) parallel to X–Z plane of the Leis Phase shows addition colours (*blue*), indicating quartz-c-axes rotated clockwise from the Z-direction (shear sense top-to-the-NE)

Phase deformation increases strongly towards the northern boundary of the Adula Nappe (Fig. 10c). Thin sections of quartzitic layers parallel to the Leis-Phase foliation show evidence for subgrain rotation recrystallization (Fig. 10d). These relations are exactly the same as in Val Scaradra and they can continuously be followed from Leis to Val Scaradra (Löw 1987). The Leis fold axis determined from the distribution of older foliations is almost identical: 055/15 in Leis and 054/19 in Val Scaradra (Figs. 4a, 10b). However, the shear sense is opposite. On rock surfaces parallel to the stretching lineation and perpendicular to the Leis-Phase foliation, shear bands and asymmetric porphyroclasts show the opposite shear sense with respect to Val Scaradra, namely top-ENE or dextral in map view (Fig. 10a). This shear sense is confirmed by microstructural criteria in X–Z thin sections, including obliquity of grain boundaries and grain-long-axes

Fig. 11 Crystallographic preferred orientation (CPO) and microstructure of quartz in sheared quartz veins from the Vals-Scaradra Shear Zone. Textures from the western part show a combination of sinistral shearing and coaxial flattening strain (particularly JK47, JK61, VF41). Photomicrograph of VF41 from the Darlun Zone shows evidence for post-kinematic annealing. The pole figures from the eastern part (V6 and V7) represent strong textures with dextral simple shear component and only minor indication of flattening. V14 from the middle of the shear zone shows flattening without a clear simple-shear component. Textures obtained by X-ray diffraction or time-of-flight neutron diffractometer and plotted in lower-hemisphere, equal-area projection. The trace of the foliation is in pole figures along the "equator" and the stretching lineation (X-direction of strain) within the foliation at the periphery, so that the Z-direction is at the *upper* and *lower vertical* extremities, and Y is in the *middle*. Thin sections (with crossed polarizers) on the *right* correspond with quartz pole figures on the *left*. Sections are orientated parallel to stretching lineation. Sample coordinates according to Swiss kilometric grid (CH1903/LV03) ▶

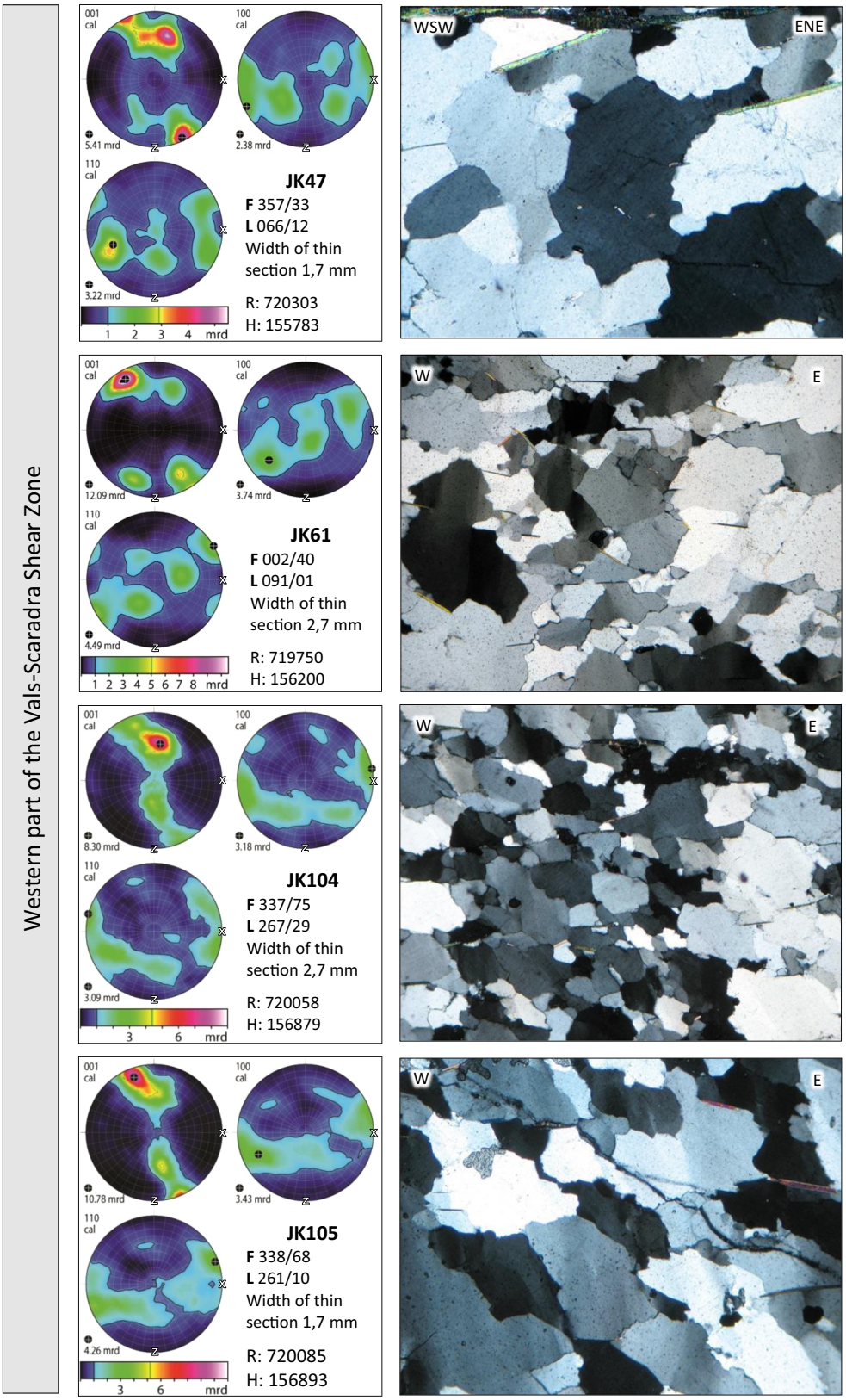
Western part of the Vals-Scaradra Shear Zone
001 cal
100 cal
110 cal
5.41 mrd
2.38 mrd
3.22 mrd
1 2 3 4 mrd
JK47
F 357/33
L 066/12
Width of thin section 1,7 mm
R: 720303
H: 155783
WSW
ENE
12.09 mrd
3.74 mrd
4.49 mrd
1 2 3 4 5 6 7 8 mrd
JK61
F 002/40
L 091/01
Width of thin section 2,7 mm
R: 719750
H: 156200
W
E
8.30 mrd
3.18 mrd
3.09 mrd
3 6 mrd
JK104
F 337/75
L 267/29
Width of thin section 2,7 mm
R: 720058
H: 156879
10.78 mrd
3.43 mrd
4.26 mrd
JK105
F 338/68
L 261/10
Width of thin section 1,7 mm
R: 720085
H: 156893

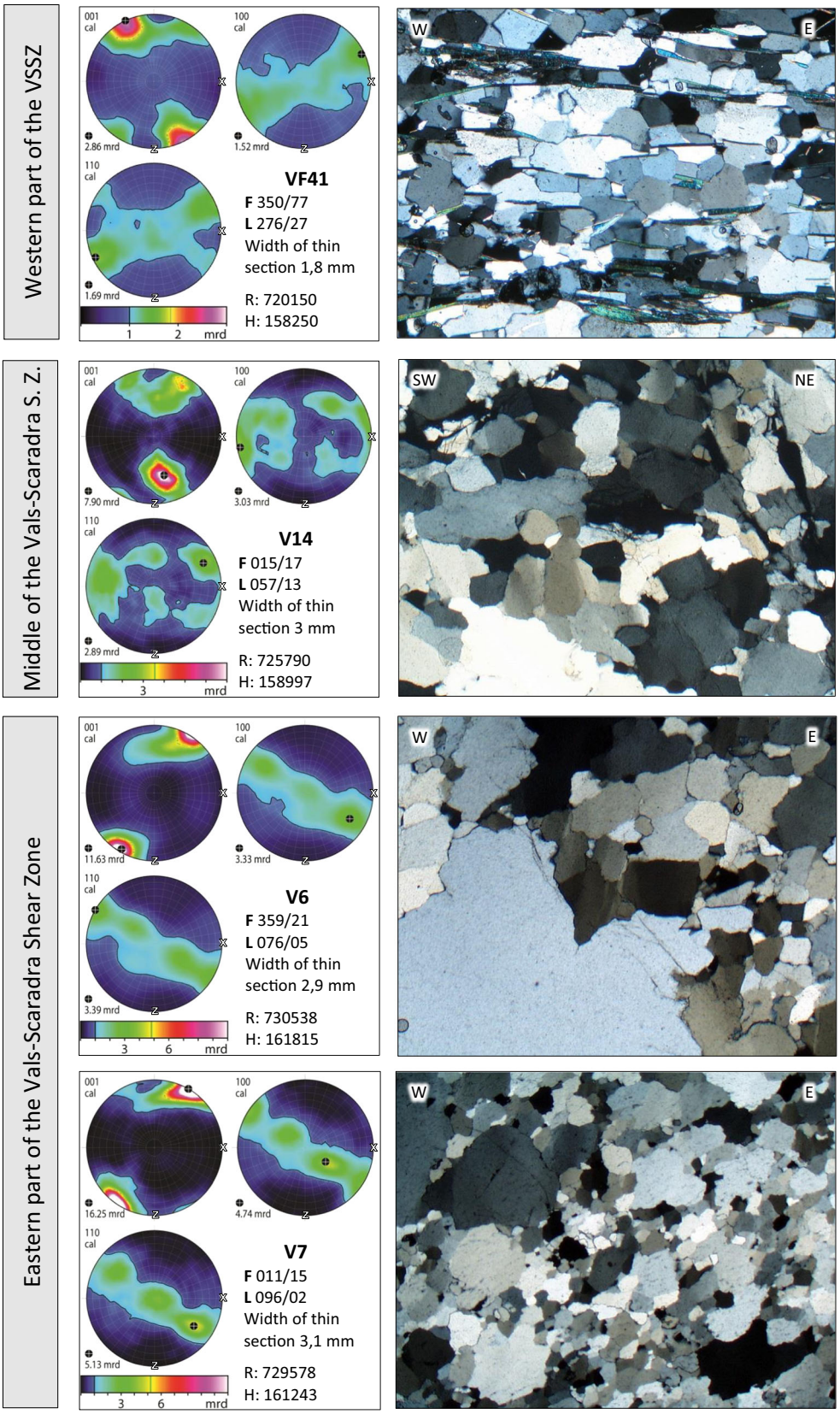

Fig. 11 continued

with respect to the main foliation (Fig. 10d), porphyroclast systems, and mica fishes. Under crossed polarizers with the gypsum plate inserted, recrystallized quartz grains in X–Z thin sections show mostly blue colours, indicating a preferred c-axis orientation rotated clockwise from the Z direction, which is evidence for dextral shearing as well (Fig. 10d).

7 Microstructure and texture of Leis-Phase quartz mylonites

Eight oriented samples of recrystallized quartz layers parallel to the foliation and bearing the stretching lineation of the Leis Phase were studied in terms of microstructure and crystallographic preferred orientation (CPO; Fig. 11). Four of the samples (JK47, JK61, JK104, JK105) are from the western part of the Adula-Nappe border, one (VF41) is from the Darlun Zone in front of it. Two samples come from the eastern part of the Adula-Nappe border (V6, V7) and one (V14) is from the middle of the Vals-Scaradra Shear Zone. The orientation of foliation and stretching lineation of this latter sample is similar to the others and we therefore assume that it also represents the Leis Phase. Sample coordinates are given in Fig. 11 and locations are indicated on the map (Fig. 12).

CPO was determined using an X-ray texture goniometer at the Department of Structural Geology and Geodynamics of Göttingen University, Germany, as well as using the time-of-flight neutron diffractometer SKAT at the Frank Laboratory of Neutron Physics in Dubna, Russia (Ullemeyer et al, 1998; Keppler et al. 2014). The three-dimensional orientation distribution function (ODF) was calculated from the measured distribution of the reflecting lattice planes using PFPlot, BEARTEX and MAUD (Lutterotti et al. 1997). Pole figures were extracted from the ODF for c-axes, denoted {001}, a-axes, denoted {110}, and normals to the trigonal prism, denoted {100}. All pole figures are oriented such that geographic east or northeast (depending on the orientation of the stretching lineation) is to the right.

7.1 Western part of the Vals-Scaradra Shear Zone

The X–Z thin sections (perpendicular to the foliation and parallel to the stretching lineation) show white mica grains oriented parallel to the foliation, partly forming asymmetric mica fishes indicating sinistral shear sense (sample VF41). Quartz grain size of the five westernmost samples is variable, with the largest grains around 1 mm and the smallest around 0.2 mm. The distribution of grain sizes is similar in all samples except VF41, which shows a smaller and relatively uniform grain size around 0.1 mm. Boundaries between quartz grains are moderately lobate. Quartz shows undulose extinction, deformation bands, and locally subgrains. Two of the four samples (JK104, JK105) show a preferred orientation of grain boundaries and grain long axes oblique to the main foliation, indicating sinistral sense of shear. In one sample (VF41 from the Darlun Zone) quartz boundaries show 120° triple junctions suggesting annealing. The microstructure of the other four samples shows locally a bimodal grain-size distribution (JK61) and suggests quartz recrystallization by subgrain rotation, which is typical for a temperature range of 400–500 °C (Stipp et al. 2002). This is in line with the temperature of ca. 500 °C determined for the Leis Phase by Löw (1987).

The textures are relatively strong for the samples inside the Adula-Nappe basement: {c} maxima, denoted {001}, are between 5.4 and 12.1 multiples of random distribution

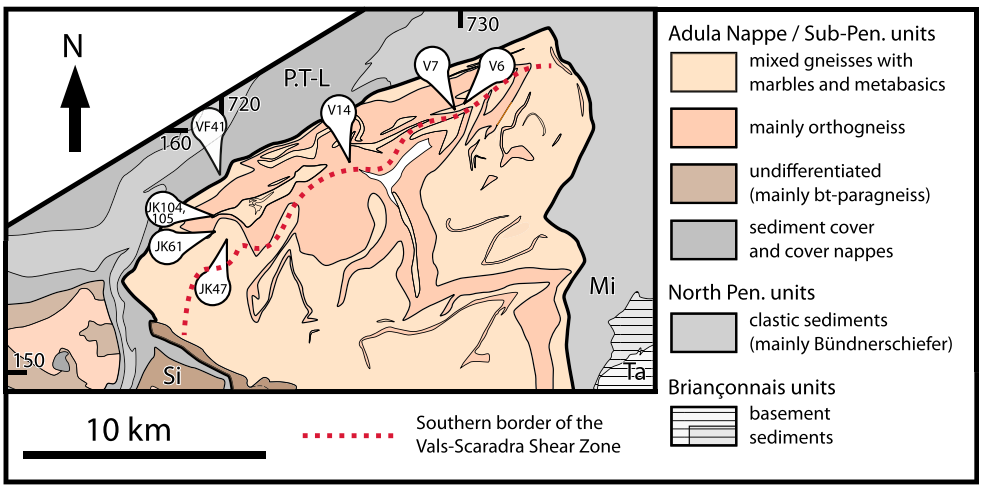

Fig. 12 Overview map with sample locations in the Vals-Scaradra Shear Zone (map after Nagel 2008). *Red dotted line* is the southern border of the area where the WSW–ENE stretching lineation of the Leis Phase occurs, i.e. the southern border of the Vals-Scaradra Shear Zone

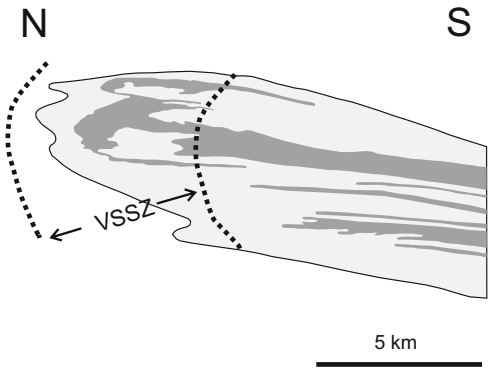

Fig. 13 Restored profile of the northern Adula Nappe after the Leis Phase and before the Carassino Phase, simplified from Cavargna-Sani et al. (2014b). *Dark grey* Zervreila orthogneiss; *light grey* all other rock types. VSSZ Vals-Scaradra Shear Zone

(mrd). The texture of VF41 is still pronounced but significantly weaker, with a {c} maximum of 2.86 mrd. This correlates with the observation of polygonalization in the microstructure of VF41: postkinematic, static annealing may have weakened the texture.

In all samples, the absolute {c} maxima are at or close to the periphery with the exception of JK104 where the maximum is ca. 45° away from the periphery. {c} maxima at the periphery indicate a predominance of basal- <a> glide, whereas the inclined maximum in JK104 may indicate a contribution of rhomb- <a> glide (e.g. Schmid and Casey 1986). In all western samples, textures show evidence for non-coaxial deformation with a sinistral, i.e. top-west shear sense. The absolute {c} maximum is rotated counterclockwise away from the Z-direction and the absolute maximum of {a}, i.e. {110}, which is the slip direction of the active glide systems, is rotated counterclockwise away from the X-direction, indicating a sinistral shear sense (e.g. Schmid and Casey 1986).

Four of the five textures show evidence for flattening strain. JK47, JK61, and VF41 have {c} maxima arranged on small circles around Z, with the strongest maximum on these girdles being the one that indicates sinistral shearing. JK105 shows a great-circle distribution of {a} close to the equator, perpendicular to the {c} maximum near Z. This, in particular, probably reflects a significant component of flattening strain because the aperture of the rudimentary {c} small circles is expected to become smaller and the aperture of the {a} small circles to become larger with increasing flattening strain (Lister and Hobbs 1980). JK104 exhibits a partial girdle of {c} oblique to the YZ plane of the pole figure, which may indicate larger strain than in the remaining samples. However, the asymmetry with respect to the sample reference frame (e.g. lineation and foliation) is lower, pointing to a smaller simple shear component.

7.2 Middle part of the Vals-Scaradra Shear Zone

The distribution of grain sizes of V14 from the middle of the northern Adula Nappe is similar to the samples from the western part. Boundaries between quartz grains are moderately lobate. Quartz shows undulose extinction, deformation bands, and subgrains. There is no clear preferred orientation of grain boundaries and grain long axes are partly perpendicular to the main foliation.

The texture of V14 shows little asymmetry. A pronounced maximum of {c} axes (>7 m.r.d.) is ~30° from the periphery in the lower part of the pole figure, only slightly rotated counterclockwise away from the Z-direction. A weaker secondary maximum of {c} axes (>4 m.r.d.) is located on a small circle around Z in the upper part of the pole figure. The texture suggests nearly coaxial flattening.

7.3 Eastern part of the Vals-Scaradra Shear Zone

The microstructures of the two samples show obvious bimodal grain-size distributions (Fig. 11; V6, V7). The large grains (>3 mm), which occupy less than half of the bulk volume, show some lobate grain boundaries pointing to grain boundary migration. This indicates temperatures of >550°. These temperatures are more typical for the earlier Zapport Phase. However, the large grains frequently show subgrains and are surrounded by recrystallized grains of a similar size as the subgrains (~0.3 mm) indicating dominant subgrain rotation recrystallization. These recrystallized grains present the largest part of the bulk volume and are obviously related to the CPO. This is also clear from the photomicrograph of Fig. 10d, which shows almost exclusively addition colours (with crossed polarizers and gypsum plate inserted).

The textures of the samples V6 and V7 are the strongest of all taken samples: {c} maxima plot at the periphery and are ~12 and ~16 mrd, respectively. The {c} maxima are rotated clockwise away from the Z-direction and yield a top-northeast to top-east shear sense. The distribution of {a}, i.e. {110}, shows girdle structure with several maxima, the strongest of which is rotated counterclockwise away from the X-direction, also indicating dextral shear sense. V7 shows a weak small girdle of {c} around Z, reminiscent of the samples in the western part but less strongly developed. The textures of V6 and V7 can be interpreted as indicating dextral simple shear with only minor flattening.

In summary, the textures from the western part of the Vals-Scaradra Shear Zone reflect a combination of flattening and sinistral shearing. The active glide systems were mostly basal- <a> and rhomb- <a>, and the recrystallization mechanism subgrain rotation, indicative of T

between 400 and 500 °C. The microstructure of the sample from the Darlun Zone outside of the Adula Nappe, VF41, exhibits the same features as the samples from inside the Adula Nappe but, in addition, shows evidence for some post-kinematic annealing, which we do not observe within the Adula Nappe. By all means, the texture of this sample is similar to the textures of samples from the Adula Nappe and shows clear evidence for the same kinematics of the Leis Phase outside the Adula-Nappe basement.

The pole figures from the eastern part of the shear zone, on the other hand, yield strong textures with clear dextral simple shear component and only minor indication of flattening. V14 represents the neutral point of the shear zone and shows flattening without a clear simple-shear component.

8 Discussion

The Vals-Scaradra Shear Zone deformed the front of the Adula Nappe and the adjacent Mesozoic metasediments during the Leis Phase. It is characterized by a foliation subparallel to the nappe boundary and fold-axis-parallel stretching lineations plunging shallowly northeast. Parallelism between fold axes and stretching direction can be achieved by rotation of originally transverse fold axes into parallelism with the stretching direction, by very large amounts of simple shear (Escher and Watterson 1974). This is unlikely here because the textures from the western part of the shear zone, in Val Scaradra, indicate a large component of flattening and only a minor rotational component of deformation. Therefore, the parallelism is more likely to result from an initial orientation of the foliation parallel to the X and Z directions of Leis-phase strain, i.e. the folds formed parallel to the X direction from the beginning (e.g., Froitzheim 1992).

In order to reconstruct the original orientation of the shear zone during its activity, the geometry prevailing at the end of the Leis Phase needs to be reconstructed by removing the effects of the Carassino Phase. For this purpose, we used the kinematic reconstruction of Cavargna-Sani et al. (2014b), shown in Fig. 13. We assumed that the southern boundary of the Vals-Scaradra Shear Zone is represented by the boundary between the area where N–S to NW–SE directed Zapport-Phase stretching lineation is dominant, and the area where WSW–ESE Leis lineation is dominant. This boundary is well defined in the field. We first located it on the map (Fig. 12), using our own results and those of Löw (1987). In a next step, we relocated the boundary on the retro deformed profile (Fig. 13). The northern boundary of the shear zone is less well constrained than the southern one. It must lie at an unknown distance north of the front of the Adula Nappe since rocks of the Piz Terri-Lunschania Zone are affected by the shear zone as well. The northern boundary in Fig. 13 is therefore hypothetic; the actual shear zone boundary may lie further north than shown here.

The reconstructed profile shows two important features. First, the Adula Nappe was inclined to the South before the Carassino Phase, in contrast to the present-day situation where it is slightly inclined to the North on N–S profiles (Fig. 2). Second, the southern boundary of the shear zone was not straight but convex to the north, similar to the frontal boundary of the Adula Nappe but with less curvature.

The along-strike shear-sense reversal implies that the Vals-Scaradra Shear Zone represents a stretching fault in the sense of Means (1989, 1990), i.e. a fault where either one of the sides or both are shortened or stretched in a direction parallel to the fault during its activity. Such faults can exhibit shear-sense reversals both in time and in space along the fault. There is no evidence for shortening of the Adula Nappe in a direction parallel to the Vals-Scaradra Shear Zone but, on the contrary, the rocks were everywhere along the front of the nappe stretched in WSW–ENE direction, as indicated by the Leis stretching lineation. Therefore, even stronger WSW–ENE stretching of the units in front of the Adula Nappe is required for the shear-sense reversal to form. On the other hand, the intensity of WSW–ESE stretching decreases southward inside the Adula Nappe. These facts put strong constraints on the flow field that affected the Adula Nappe during the Leis Phase. A simple flow field fulfilling these constraints is qualitatively shown in Fig. 14. A neutral point is in the middle of the nappe front, where the shear sense changes from dextral to sinistral. This is taken as the reference point for the displacement arrows. The rocks outside the Adula Nappe move away from the neutral point in a direction parallel to the nappe front, just like the ones inside the Adula Nappe. However, the rocks outside must have moved at higher rates than the inside ones in order to explain the observed

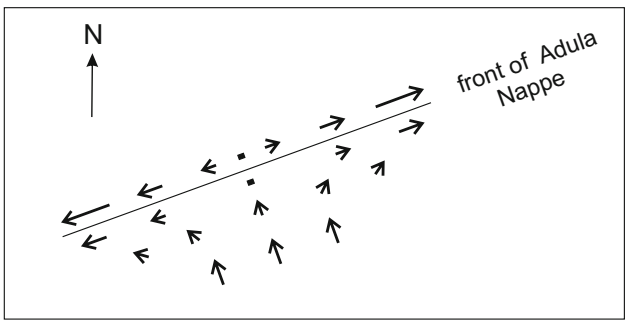

Fig. 14 Schematic and qualitative sketch of the low field during the Leis Phase at the front of the Adula Nappe. *Length of arrows* is related to displacement rate relative to the two points. For further explanation, see text

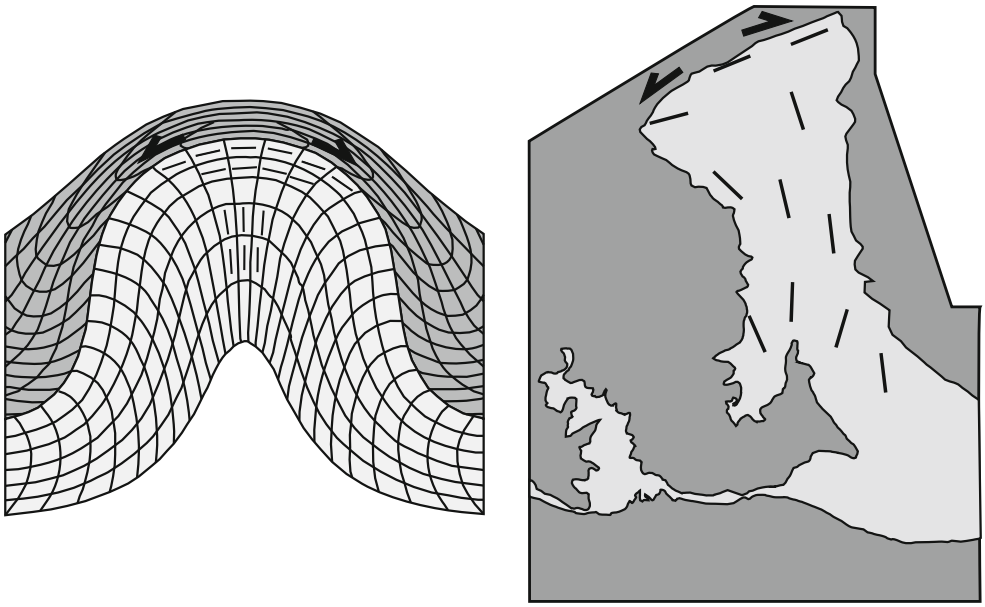

Fig. 15 *Left side* Cross-section through centrifuge analogue model WD-4 of Dixon (1975), consisting of a lower layer (*light grey*) with lower density and higher viscosity, and an upper layer (*dark grey*) with higher density and lower viscosity. Deformation of initially *square grid* shows strain and shear sense. Within the diapir, the direction of stretching is indicated by short black lines. It is vertical in the lower part and horizontal in the upper part of the diapir. Above the top of the diapir, shear sense is indicated by *black half arrows*. *Right side* Orientation of stretching lineation in the Adula Nappe after Nagel (2008). N–S to NW–SE trending stretching lineations formed during the Zapport Phase, WSW–ENE stretching lineations at the front of the Adula Nappe during the Leis Phase. Shear sense in the Vals-Scaradra Shear Zone indicated by *half arrows*

shear senses. Further south in the Adula Nappe, the displacement arrows must have a component directed towards the nappe front in order to accommodate shortening perpendicular and stretching parallel to the nappe front. Still further south, there is no evidence for WSW–ENE stretching, i.e. the displacement vectors must become parallel to each other and perpendicular to the nappe front.

The deformation in the Vals-Scaradra Shear Zone, i.e., the Leis Phase, occurred during near-isothermal decompression (Löw 1987), as was the case for the preceding Zapport Phase. The activity of the shear zone resulted in a temperature contrast of ca. 100 °C across the front of the Adula Nappe (Wiederkehr et al. 2011). The flow field shown in Fig. 14 is able to explain these observations: The flow in the interior of the Adula Nappe was directed towards the nappe front and the nappe was inclined to the south, which means that the rocks were exhumed, and heat was advected to the nappe front by the exhuming rocks.

The Leis-Phase flow field is similar to the one at the head of a diapir (e.g., Dixon 1975; Fig. 15). In the following, we will discuss similarities between the Adula Nappe and diapiric rise. It is important to note that we discuss diapiric rise in the sense of a purely kinematic concept that does not imply anything about the dynamics of the exhumation during the Leis Phase, e.g. buoyancy is not necessarily considered a driving force. Figure 15 shows the results of a centrifuge analogue model of (in fact buoyancy-driven) diapir formation by Dixon (1975). The figure is a vertical section through an experiment with a cylindrical geometry. Of the two layers shown, the lower one had a lower density and a higher viscosity of 1.5×10^5 Pa.s. The upper, higher-density layer had a viscosity of 3.49×10^4 Pa.s. Deformation of an originally square grid visualizes the strain. The rise of the diapir led to sideward extrusion of the upper layer, the boundary between the two layers being a shear zone with sinistral shear sense to the left and dextral shear sense to the right. The black lines show the long axis of strain within the diapir, vertical at a deeper level and horizontal, parallel to the front, at the top of the diapir. Comparing the model with the overall geometry and finite strain field of the Adula Nappe reveals several similarities: (1) In the frontal part of the diapir, the direction of maximum stretching is horizontal and parallel to the boundary; (2) horizontal stretching decreases away from the boundary; (3) in the low-viscosity material in front of the diapir, stretching is also parallel to the boundary but stronger than inside, leading to a shear-sense reversal from sinistral shearing to the left to dextral shearing to the right, as indicated by shear-sense arrows (black half arrows).

The analog model of Dixon (1975) differs from most other diapir models in that the diapir material is given a higher viscosity than the overlying material. This is different from salt diapirs, which have much lower viscosity than the overlying material. The viscosity contrast in the model may, however, be similar to the

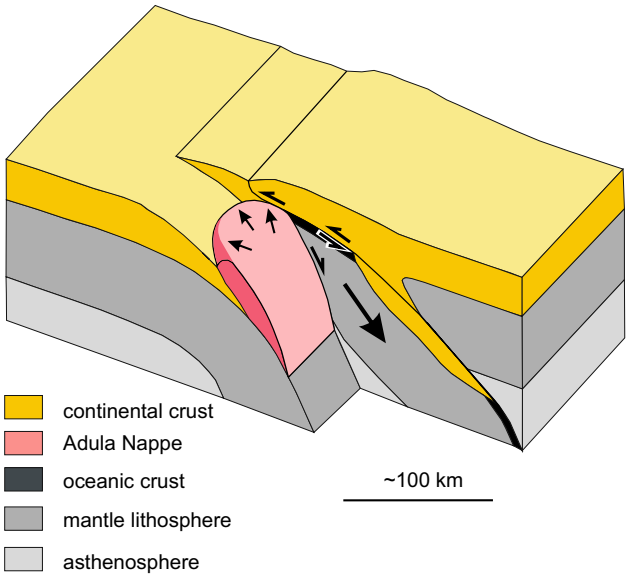

Fig. 16 Block diagram schematically depicting the exhumation of the Adula Nappe from the Valaisan subduction zone during extraction of the Piemont-Ligurian/Briançonnais slab. N–S profile is after Froitzheim et al. (2003). For further explanation see text

case of the Adula Nappe where the interior of the nappe is mainly gneiss and the exterior mainly carbonate-bearing schist.

An important difference between the model and the actual situation at the front of the Adula Nappe is that the model diapir has a cylindrical geometry, i.e. the stretching direction at the front is radially away from the centre, whereas it is consistently WSW–ENE at the front of the Adula Nappe. In the case of the Adula Nappe, the flow was not radial in all directions but confined between two "walls". Figure 16 shows a possible tectonic framework of such a confined flow, based on a cross-section from Froitzheim et al. (2003). It is assumed that the exhumation of the Adula Nappe occurred in a three-plate, two-subduction-zone scenario where the downward extraction of the middle plate (Piemont-Ligurian Ocean and Briançonnais microcontinent) released the subducted Adula Nappe from the northern subduction zone. During its rise, the Adula Nappe expelled the metasediments ahead of its front towards east and west and assumed a tongue-like geometry, leading to the strain and shear sense described above.

As already mentioned, a problem in this and other exhumation models is that the rise of the Adula Nappe from the subduction channel should have led to top-South shearing in the roof of the nappe which is not observed. Instead, the shear sense of mylonites along the roof of the nappe is generally top-North. This shear sense may be explained by the kinematic framework shown in Fig. 16: The sense of shearing along the roof of the Adula Nappe is different on both sides of the tip of the extracted slab; top-South below and top-North above, as indicated by arrows in Fig. 16. As the extracted slab moves down and the Adula Nappe up, the Adula rocks pass by the tip of the slab and earlier top-south mylonites could become overprinted by top-North shearing. This is the situation described as "mixed extraction fault" by Froitzheim et al. (2006). A detailed study of strain, microstructure, and texture in mylonites of the Adula Nappe could test this hypothesis.

9 Conclusions

The front of the Adula Nappe and the adjacent metasediments were deformed by the newly described Vals-Scaradra Shear Zone. It was active during the Leis Phase and is characterized by orogen-parallel stretching, a shear-sense reversal along strike, and a drop of metamorphic peak temperature across the nappe front. The shear sense reversal is confirmed by quartz textures. The kinematics of deformation are explained in the following way: The Adula basement protruded upward and northward into the metasediments, spread laterally, and expelled the metasediments in its front towards west and east. Advection of heat to the laterally spreading nappe front explains the temperature drop across it. The model could be tested by further structural studies both within the Adula Nappe and in the enveloping units.

Acknowledgements We thank Michael Wiederkehr, Neil Mancktelow, and editor Stefan Schmid for careful and constructive reviews. We are grateful to the Frank Laboratory of Neutron Physics (FLNP) in Dubna (Russia) for supporting the neutron diffraction texture measurements. We also would like to thank Rebecca Kühn for her help with the X-ray diffraction texture measurements.

References

Becker, H. (1993). Garnet peridotite and eclogite Sm-Nd mineral ages from the Lepontime dome (Swiss Alps): New evidence for Eocene high-pressure metamorphism in the central Alps. *Geology, 21,* 599–602.

Berger, A., Mercolli, I., & Engi, M. (2005). The Central Lepontine Alps: Notes accompanying the tectonic and petrographic map sheet Sopra Ceneri (1:100'000). *Schweizerische Mineralogische und Petrographische Mitteilungen, 85,* 109–146.

Brenker, F. E., & Brey, G. P. (1997). Reconstruction of the exhumation path of the Alpe Arami garnet-peridotite body from depths exceeding 160 km. *Journal of Metamorphic Geology, 15,* 58–592.

Brouwer, F. M., Burri, T., Engi, M., & Berger, A. (2005). Eclogite relics in the Central Alps: PT-evolution, Lu–Hf ages and implications for formation of tectonic mélange zones. *Schweizerische Mineralogische und Petrographische Mitteilungen, 85,* 147–174.

Cavargna-Sani, M., Epard, J.-L., Bussy, F., & Ulianov, A. (2014a). Basement lithostratigraphy of the Adula nappe: implications for Palaeozoic evolution and Alpine kinematics. *International Journal of Earth Sciences, 103,* 61–82.

Cavargna-Sani, M., Epard, J. L., & Masson, H. (2010). Discovery of fossils in the Adula nappe, new stratigraphic data and tectonic consequences (Central Alps). *Bulletin de la Société vaudoise des Sciences naturelles, 92,* 77–84.

Cavargna-Sani, M., Epard, J.-L., & Steck, A. (2014b). Structure, geometry and kinematics of the northern Adula nappe (Central Alps). *Swiss Journal of Geosciences, 107,* 135–156.

Dale, J., & Holland, T. J. B. (2003). Geothermobarometry, P–T paths and metamorphic field gradients of high-pressure rocks from the Adula Nappe, Central Alps. *Journal of Metamorphic Geology, 21,* 813–829.

Dixon, J. M. (1975). Finite strain and progressive deformation in models of diapiric structures. *Tectonophysics, 28,* 89–124.

Escher, A., & Watterson, J. (1974). Stretching fabrics, folds and crustal shortening. *Tectonophysics, 22,* 223–231.

Froitzheim, N. (1992). Formation of recumbent folds during synorogenic crustal extension (Austroalpine nappes, Switzerland). *Geology, 20,* 923–926.

Froitzheim, N., Pleuger, J., & Nagel, T. J. (2006). Extraction faults. *Journal of Structural Geology, 28,* 1388–1395.

Froitzheim, N., Pleuger, J., Roller, S., & Nagel, T. (2003). Exhumation of high- and ultrahigh-pressure metamorphic rocks by slab extraction. *Geology, 31,* 925–928.

Galster, F., Cavargna-Sani, M., Epard, J.-L., & Masson, H. (2012). New stratigraphic data from the Lower Penninic between the Adula nappe and the Gotthard massif and consequences for the tectonics and the paleogeography of the Central Alps. *Tectonophysics, 579,* 37–55. doi:10.1016/j.tecto.2012.05.029.

Galster, F., Epard, J.-L., & Masson, H. (2010). The Soja and Luzzone-Terri nappes: Discovery of a Briançonnais element below the front of the Adula nappe (NE Ticino, Central Alps). *Bulletin de la Société Vaudoise des Sciences Naturelles, 92,* 61–75.

Gebauer, D. (1996). A P–T-t path for an (ultra?-) high-pressure ultramafic/mafic rock-association and its felsic country-rocks based on SHRIMP-dating of magmatic and metamorphic zircon domains. Example: Alpe Arami (Central Swiss Alps). In A. Basu & S. Hart (Eds.), *Earth processes: Reading the isotopic code, Geophysical Monograph, 95* (pp. 307–330). Washington: American Geophysical Union.

Heinrich, C. A. (1986). Eclogite facies regional metamorphism of hydrous mafic rocks in the Central Alpine Adula Nappe. *Journal of Petrology, 27,* 123–154.

Herwartz, D., Nagel, T. J., Münker, C., Scherer, E. E., & Froitzheim, N. (2011). Tracing two orogenic cycles in one eclogite sample by Lu-Hf garnet chronometry. *Nature Geoscience, 4,* 178–183. doi:10.1038/NGEO1060.

Jenny, H., Frischknecht, G., & Kopp, J. (1923). Geologie der Adula. *Beiträge zur Geologischen Karte der Schweiz N.F., 51,* 1–123.

Keppler, R., Ullemeyer, K., Behrmann, J. H., & Stipp, M. (2014). Potential of full pattern fit methods for the texture analysis of geological materials: Implications from texture measurements at the recently upgraded neutron time-of-flight diffractometer SKAT. *Journal of Applied Crystallography*. doi:10.1107/S1600576714015830.

Liati, A., Gebauer, D., & Fanning, C. M. (2009). Geochronological evolution of HP metamorphic rocks of the Adula nappe, Central Alps, in pre-Alpine and Alpine subduction cycles. *Journal of the Geological Society, 166,* 797–810.

Lister, G. S., & Hobbs, B. E. (1980). The simulation of fabric development during plastic deformation and its application to quartzite: The influence of deformation history. *Journal of Structural Geology, 2,* 355–370.

Löw, S. (1987). Die tektono-metamorphe Entwicklung der Nördlichen Adula-Decke. *Beiträge zur Geologischen Karte der Schweiz N.F., 161,* 1–84.

Lutterotti, L., Matthies, S., Wenk, H.-R., Schultz, A. J., & Richardson, J. W. (1997). Combined texture and structure analysis of deformed limestone from time-of-flight neutron diffraction spectra. *Journal of Applied Physics, 81,* 594–600.

Means, W. D. (1989). Stretching faults. *Geology, 17,* 893–896.

Means, W. D. (1990). One-dimensional kinematics of stretching faults. *Journal of Structural Geology, 12,* 267–272.

Meyre, C., & Puschnig, A. R. (1993). High-pressure metamorphism and deformation at Trescolmen, Adula nappe, Central Alps. *Schweizerische Mineralogische und Petrographische Mitteilungen, 73,* 277–283.

Nagel, T. J. (2008). Tertiary subduction, collision and exhumation recorded in the Adula nappe, central Alps. In S. Siegesmund, B. Fügenschuh, & N. Froitzheim (Eds.), *Tectonic Aspects of the Alpine-Dinaride-Carpathian System* (298th ed., pp. 365–392). London, Special Publication: Geological Society.

Nagel, T., de Capitani, C., & Frey, M. (2002a). Isograds and P–T evolution in the eastern Lepontine Alps (Graubünden, Switzerland). *Journal of Metamorphic Geology, 20,* 309–324.

Nagel, T., de Capitani, C., Frey, M., Froitzheim, N., Stünitz, H., & Schmid, S. M. (2002b). Structural and metamorphic evolution during rapid exhumation in the Lepontine dome (southern Simano and Adula nappes, Central Alps, Switzerland). *Eclogae Geologicae Helvetiae, 95,* 301–321.

Nimis, P., & Trommsdorff, V. (2001). Revised thermobarometry of Alpe Arami and other garnet peridotites from the Central Alps. *Journal of Petrology, 42,* 103–115.

Pleuger, J., Hundenborn, R., Kremer, K., Babinka, S., Kurz, W., Jansen, E., et al. (2003). Structural evolution of Adula nappe, Misox zone, and Tambo nappe in the San Bernardino area: Constraints for the exhumation of the Adula eclogites. *Mitteilungen der Österreichischen Geologischen Gesellschaft, 94,* 99–122.

Pleuger, J., Nagel, T.J., Walter, J.M., Jansen, E., Froitzheim, N. (2008). On the role and importance of orogen-parallel and-perpendicular extension, transcurrent shearing, and backthrusting in the Monte Rosa nappe and the Southern Steep Belt of the Alps (Penninic zone, Switzerland and Italy). In S. Siegesmund, B. Fügenschuh, N. Froitzheim (Eds.), *Tectonic Aspects of the Alpine-Dinaride-Carpathian System.* Geological Society, London, Special Publication 298 (pp. 251–280).

Pleuger, J., & Podladchikov, Y. Y. (2014). A purely structural restoration of the NFP20-East cross section and potential tectonic overpressure in the Adula nappe (central Alps). *Tectonics, 33,* 656–685. doi:10.1002/2013TC003409.

Probst, P. (1980). Die Bündnerschiefer des nördlichen Penninikums zwischen Valser Tal und Passo di San Giacomo. *Beiträge zur Geologischen Karte der Schweiz N.F., 153,* 1–64.

Sandmann, S., Nagel, T. J., Herwartz, D., Fonseca, R. O. C., Kurzawski, R. M., Münker, C., et al. (2014). Lu–Hf garnet systematics of a polymetamorphic basement unit: new evidence for coherent exhumation oft he Adula Nappe (Central Alps) from eclogite-facies conditions. *Contributions to Mineralogy and Petrology, 168,* 1–21. doi:10.1007/s00410-014-1075-6.

Schmid, S. M., & Casey, M. (1986). Complete fabric analysis of some commonly observed quartz c-axis patterns: Mineral and rock deformation. *American Geophysical Union, Geophysical Monograph, 36,* 263–286.

Schmid, S. M., Pfiffner, O. A., Froitzheim, N., Schönborn, G., & Kissling, E. (1996). Geophysical-geological transect and tectonic evolution of the Swiss-Italian Alps. *Tectonics, 15,* 1036–1064.

Stipp, M., Stünitz, H., Heilbronner, R., & Schmid, S. M. (2002). The eastern Tonale fault zone: A 'natural laboratory' for crystal plastic deformation of quartz over a temperature range from 250 to 700 C. *Journal of Structural Geology, 24,* 1861–1884.

Trommsdorff, V. (1993). Metamorphism and tectonics in the Central Alps: The Alpine lithospheric mélange of Cima Lunga and Adula. *Memorie della Società Geologica Italiana, 45*(1990), 39–49.

Ullemeyer, K., Spalthoff, P., Heinitz, J., Isakov, N. N., Nikitin, A. N., & Weber, K. (1998). The SKAT texture diffractometer at the pulsed reactor IBR-2 at Dubna: Experimental layout and first measurements. *Nuclear Instruments and Methods of Physical Research, 412,* 80–88.

Voll, G. (1976). Structural studies of the Valser Rhine valley and the Lukmanier region and their importance for the nappe structure of the Central Swiss Alps. *Schweizerische Mineralogische und Petrographische Mitteilungen, 56,* 619–626.

Wiederkehr, M., Bousquet, R., Schmid, S.M., Berger, A. (2008). From subduction to collision: Thermal overprint of HP/LT metasediments in the north-eastern Lepontine Dome (Swiss Alps) and consequences regarding the tectono-metamorphic evolution of the Alpine orogenic wedge. In N. Froitzheim & S.M. Schmid (Eds.) *Orogenic processes in the Alpine collision zone. Swiss Journal of Geosciences, 101* (pp. 127–155).

Wiederkehr, M., Bousquet, R., Ziemann, M. A., Berger, A., & Schmid, S. M. (2011). 3-D assessment of peak-metamorphic conditions by Raman spectroscopy of carbonaceous material: an example from the margin of the Lepontine dome (Swiss Central Alps). *International Journal of Earth Sciences, 100,* 1029–1063. doi:10.1007/s00531-010-0622-2.

Wiederkehr, M., Sudo, M., Bousquet, R., Berger, A., & Schmid, S. M. (2009). Alpine orogenic evolution from subduction to collisional thermal overprint: the $^{40}Ar/^{39}Ar$ age constraints from the Valaisan Ocean, Central Alps. *Tectonics, 28,* 1–28. doi:10.1029/2009TC002496.

Zulbati, F. (2008). Structural and metamorphic evolution of the phengite-bearing schists of the northern Adula Nappe (Central Alps, Switzerland). *Geological Journal, 43,* 33–57.

Zulbati, F. (2011). Multistage metamorphism and deformation in high-pressure metabasites of the northern Adula Nappe Complex (Central Alps, Switzerland). *Geological Journal, 46,* 82–103.